34p

NASA TN D-1774

N63-15771
code-1

NASA TN D-1774

TECHNICAL NOTE

D-1774

AERODYNAMIC CHARACTERISTICS OF A FULL-SCALE PROPELLER

TESTED WITH BOTH RIGID AND FLAPPING BLADES

AND WITH CYCLIC PITCH CONTROL

By Kenneth W. Mort and Paul F. Yaggy

Ames Research Center
Moffett Field, Calif.

NATIONAL AERONAUTICS AND SPACE ADMINISTRATION

WASHINGTON May 1963

554587

44p

Code-1

NATIONAL AERONAUTICS AND SPACE ADMINISTRATION

TECHNICAL NOTE D-1774

AERODYNAMIC CHARACTERISTICS OF A FULL-SCALE PROPELLER TESTED WITH BOTH RIGID AND FLAPPING BLADES AND WITH CYCLIC PITCH CONTROL

By Kenneth W. Mort and Paul F. Yaggy

SUMMARY

15771

Basic aerodynamic characteristics of the two propeller configurations are presented for free-stream velocities ranging from 0 to 140 knots and for angles of attack ranging from 0° to 70°. The differences in the characteristics of the two configurations were small.

The effect of the cyclic pitch control on the aerodynamic characteristics and on the blade flapwise bending and trailing-edge tensile stress was examined at free-stream velocities ranging from 0 to 60 knots. The cyclic pitch control was about a single control axis, intended only to produce longitudinal trim and control. At hover conditions the cyclic control effectiveness of the rigid configuration was about twice that of the flapping configuration. By extrapolating the test results to conditions of maximum allowable blade stress it was estimated that the maximum longitudinal control capability as limited by the allowable blade stresses was greater for the rigid configuration than for the flapping configuration.

INTRODUCTION

During low-speed flight, tilting-propeller VTOL aircraft require more longitudinal control than is normally supplied from the horizontal tail. One means for providing additional longitudinal control is to vary the propeller blade angle sinusoidally. The mechanism which varied the blade angle in the present tests tilted the propeller swash plate about a single axis and was therefore called a monocyclic blade angle control. The propeller could be operated in either a flapping or a rigid configuration.

The objectives of the tests were: (1) to determine the effectiveness of monocyclically varying the blade angle for longitudinal control, (2) to compare the basic aerodynamic characteristics of the same propeller in a flapping and in a rigid configuration, and (3) to examine briefly the blade stresses resulting

from monocyclically varying the blade angle so that limits on the longitudinal control moment imposed by these stresses could be estimated.

NOTATION

b propeller blade chord, ft

B number of blades

C_D $\frac{\text{wing alone drag}}{(\text{wing area})q}$

C_L $\frac{\text{wing alone lift}}{(\text{wing area})q}$

C_m pitching-moment coefficient, $\frac{M}{\rho n^2 D^5}$

C_m' pitching-moment coefficient of wing-propeller combination, $\frac{M'}{\rho n^2 D^5}$

C_{m_w} $\frac{\text{wing alone pitching moment}}{(\text{wing area})(\text{wing chord})q}$

C_N normal-force coefficient, $\frac{N}{\rho n^2 D^4}$

C_P power coefficient, $2\pi C_Q$

C_Q propeller torque coefficient, $\frac{\text{propeller torque}}{\rho n^2 D^5}$

C_S side-force coefficient, $\frac{S}{\rho n^2 D^4}$

C_T thrust coefficient, $\frac{T}{\rho n^2 D^4}$

C_Y yawing-moment coefficient, $\frac{Y}{\rho n^2 D^5}$

D propeller diameter, ft

h maximum thickness of propeller blade section, ft

J' propeller advance ratio based on the velocity component normal to the propeller disk, $\frac{V_\infty \cos \alpha}{nD}$

M propeller pitching moment, ft-lb

M' pitching moment of wing-propeller combination, ft-lb

n propeller rotational speed, rps

N propeller normal force, lb

q free-stream dynamic pressure, lb/ft^2

r propeller blade section radius, ft

R propeller tip radius, ft

S propeller side force, lb

T propeller thrust, lb

V_∞ free-stream velocity, knots

Y propeller yawing moment, ft-lb

α angle of attack measured from the longitudinal tunnel axis to the propeller shaft axis, deg

β collective propeller blade angle measured at 0.75 R, deg; flapping configuration measured with 0° coning angle; rigid configuration measured with 1.275° coning angle

γ monocyclic blade angle; represents a once-per-revolution sinusoidal variation of blade angle relative to the collective blade angle, deg, phased as indicated in figure 4

ρ mass density of air, slugs/cu ft

σ_e weighted propeller solidity, $\frac{B}{\pi R} \frac{\int_0^R br^2\,dr}{\int_0^R r^2\,dr}$

Ω azimuth angle, deg

The positive directions of the propeller forces and moments are indicated in figure 1.

MODEL AND APPARATUS

Testing Apparatus

The propeller was mounted on the propeller test stand in the Ames 40- by 80-Foot Wind Tunnel, as shown in figure 2. On this stand, the wind shroud is

isolated from the wind-tunnel balance system so that only propeller forces and moments are measured. The angle of the thrust axis could be varied continously from 0° to 85°.

Propeller

In every respect, except the following, the propeller was a duplicate of those used on the VZ-2 airplane and of propeller number 3 in reference 1: (1) the over-all diameter had been increased from 9.5 to 9.67 feet; (2) a monocyclic mechanism had been added to the swash plate control; and (3) the blade had been strengthened to allow for the expected increase in blade stresses resulting from the monocyclic variations in blade angle by modifying the spar structure and increasing the strength of the blade grip fitting in a manner which did not significantly alter the aerodynamic characteristics. The propeller could be tested in a rigid or a flapping configuration by adding or removing locking plates across the flapping hinges. For the rigid configuration the blades were locked at a coning angle of 1.275° with respect to the plane of rotation. For the flapping configuration the flapping hinge axis was positioned so that for every degree of forward flapping or coning the blade angle was reduced by 0.34°. The physical characteristics of the propeller are listed in the following table.

Diameter	9.67 ft
Number of blades	3
Blade construction	Wood and steel
Airfoil section	NACA 0009
Activity factor/blade	178
Flapping-hinge offset	3 in.

Blade plan-form curves are presented in figure 3.

Monocyclic Blade Angle Control

In contrast with the conventional helicopter cyclic control which tilts the swash plate about two axis to generate a moment at any azimuth position, the monocyclic control tilts the swash plate about only one axis to generate a moment at a single azimuth position. It was intended that this axis be positioned for each of the two configurations so as to produce a pitching moment (i.e., moment in the 0°-180° plane). Because of the differences in the inertia and rigidity of the flapping and rigid system, the position of the maximum control input differed and was as shown in figure 4. One degree of monocyclic blade angle control represents a once-per-revolution sinusoidal variation between ±1° of blade angle relative to the collective blade angle.

Wing

During a portion of the testing a wing was mounted on the test stand in such a manner that the forces on the propeller and wing together were recorded. The wing was not attached to the shroud which is isolated from the wind-tunnel balance system. A diagram showing the geometry and position of the wing is presented in figure 5 and the wing is shown mounted on the test stand in figure 2.

Instrumentation

The propeller blades were equipped with strain gages which permitted monitoring of the critical blade stresses. The locations of these strain gages, shown in figure 6, were those at which the propeller manufacturer stated maximum stresses occurred.

Power input to the propeller was measured by means of wattmeters which were calibrated for drive system losses and, hence, indicated the net power input to the propeller.

Six-component force data were measured by the wind-tunnel balance system upon which the test stand was mounted.

TESTS

Static Tests

Data for conditions of zero advance ratio were obtained with the test stand at the maximum angle of attack of 85°, as shown in figure 2, and the tunnel access doors (essentially the entire upper half of the test section) open to a large enclosure which formed a plenum chamber. The propeller was sufficiently far removed from the floor so that there was no appreciable ground effect.

Tests at Forward Velocities

These tests were conducted at a constant rotational velocity of 1,410 rpm. The basic aerodynamic characteristics were examined at angles of attack ranging from 0° to 70°, at collective blade angles varying from 6° to 27°, and at forward velocities ranging from 20 to 140 knots. The aerodynamic characteristics at various monocyclic blade angles were examined at the following three combinations of thrust-axis angle of attack and tunnel forward velocity.

V, knots	20	40	60
α, deg	70	50	30

These conditions approximately represent trimmed, level, unaccelerated flight conditions for the Vertol 76 (VZ-2) vertical take off and landing (VTOL) aircraft.

REDUCTION OF DATA

Unless otherwise noted, the moment center for the data presented is located at the propeller hub center.

Corrections

No corrections for tunnel-wall constraint have been applied to the data. However, these corrections are believed to be small because of the large ratios of tunnel cross-sectional area to propeller disk area. Flow surveys at the plane of the propeller (propeller removed) indicated no significant induced in-flow angles due to the presence of the test stand shroud; hence, no stream-angle corrections were applied.

The collective and cyclic blade angles for the flapping configuration were not corrected for the effects of the δ_3 flapping hinge. Such corrections can be applied by reducing the indicated local blade angle by 0.34° for every 1° of indicated forward coning or flapping. If a more accurate comparison is desired between the flapping and rigid configuration, this correction would be necessary. Sufficient coning and flapping data are presented so that the correction can be performed assuming a sinusoidal variation of the flapping angle.

Stress Data

The stress data have been presented as ratios of the measured stress to the allowable stress. The manufacturer tested the blades and specified the allowable stresses for infinite blade life and for continuous operation at the maximum test disk loading. The allowable blade stresses specified were 35,000 psi for the steady flapwise bending, ±25,000 psi for the oscillating flapwise bending, 52,000 psi for the steady trailing-edge tension, and ±7,200 psi for the oscillating trailing-edge tension.

RESULTS AND DISCUSSION

Aerodynamic Characteristics

The basic aerodynamic characteristics of the flapping and rigid configuration are shown in figures 7 and 8. Figure 7 shows the figure of merit as a function of the weighted thrust coefficient (scatter resulted from the low sensitivity of the power measuring device). Figure 8 shows the variation of the basic power, force,

and moment coefficients as functions of advance ratio for several angles of attack and several collective blade angles. It is apparent from these figures that the differences in the basic aerodynamic characteristics of the two configurations are small. The thrust and power data obtained for the flapping configuration differ from the results presented in reference 1; the data in figures 7 and 8 of the present report are correct.

The variations of the power, force, and moment coefficients with monocyclic blade angle are presented for the flapping and the rigid configurations in figures 9 and 10, respectively. The results presented are for four combinations of free-stream velocity and angle of attack which represent approximate trim conditions during transition flight for the Vertol VZ-2 aircraft. For the range of conditions examined, the variations of the power and force coefficients with monocyclic blade angle are small. The magnitude of both moment coefficients is small and for this reason the moment results are presented to a rather large scale to facilitate examination of the approximately linear variations with monocyclic blade angle. (This, of course, magnifies the scatter of the data and the separation between the curves for the various blade angles.)

As expected, figures 9 and 10 show that the variation of the pitching moment about the hub center with monocyclic blade angle is much greater for the rigid configuration than for the flapping configuration. Examination of the yawing-moment results indicates that for the rigid configuration the variation of yawing-moment coefficient with monocyclic blade angle is negligible; whereas, for the flapping configuration it is relatively large. This indicates that even at the hover condition where the flapping motion is not affected by forward velocity the maximum monocyclic blade angle did not occur at the proper azimuth position to produce a pure longitudinal control moment, as was intended, for the flapping configuration. A more equitable comparison of the two configurations would be obtained by comparing the resultant of the yawing and pitching moments as produced by variations in the monocyclic blade angle. (This assumes that the magnitude of the resultant moment would not change with the azimuth angle of the monocyclic blade angle input.) When this is done the effectiveness of the monocyclic control to produce changes in the pitching moment on the flapping configuration is about one half that produced by the rigid configuration at hover.

Figures 9 and 10 also show small variations of normal-force coefficient with monocyclic blade angle for the flapping configuration, whereas for the rigid configuration these variations are negligible. However, the normal-force coefficient only changes on the average of about 0.001 for a 1° change in monocyclic blade angle. Hence, a longitudinal shift of the center-of-gravity location of one propeller diameter would be required to give an increment in C_m of only 0.001.

Thus, it may be concluded that, generally, the rigid configuration is more effective in producing changes in pitching moment by monocyclically varying the blade angle.

Effect of Monocyclic Blade Angle Variation on the Pitching-Moment Coefficient With a Wing in the Slipstream

Variations in the monocyclic blade angle will cause variations in the inclinations of the propeller slipstream. Therefore, the contribution to the pitching moment by bodies immersed in the slipstream may vary with monocyclic blade angle. This effect was investigated by means of tests with a wing mounted in the slipstream. The basic aerodynamic characteristics of the wing employed are presented in figure 11 and the angle-of-attack and free-stream conditions at which this investigation was conducted are shown in figure 12(a). (These conditions approximate the angle of attack required for level unaccelerated flight for the Vertol VZ-2 and are presented here for convenient reference.) Figures 12(b), (c), and (d) show $dC_m'/d\gamma$ as a function of the free-stream velocity[1] for the center of gravity located at the hub with the wing off, for the center of gravity located at the wing quarter chord with the wing off, and for the center of gravity located at the wing quarter chord with the wing on. It is apparent from these results that the presence of the wing affected the longitudinal control produced by monocyclic blade angle variations ($dC_m'/d\gamma$) by less than 0.0005 for the range of velocities and center-of-gravity locations examined.

Flapping Configuration Blade Motion Due to Monocyclic Blade Angle Variations

Figure 13 shows the variation of coning angle with monocyclic blade angle for several collective blade angles at the conditions of figure 12(a). It is apparent from this figure that the variation of coning angle with monocyclic blade angle was small regardless of collective blade angle.

The variation of flapping angle with monocyclic blade angle for several collective blade angles is presented in figure 14. Since the motion was sinusoidal, it was convenient to show only the phase angle and amplitude in polar form. Each vector represents the flapping angle and is labeled with the value of the monocyclic blade angle input. The variations of the phase angle and amplitude of the flapping motion with monocyclic blade angle and free-stream velocity are seen to be consistent with the variations in the resultant moment inferred from the yawing- and pitching-moment-coefficient data shown in figure 9.

---

[1]As was noted in the discussion of figures 9 and 10, it was found that the variation of pitching-moment coefficient with monocyclic blade angle was linear. Therefore, to more readily examine the effect of the wing on the variation of pitching-moment coefficient with monocyclic blade angle, only the slopes, that is, $dC_m'/d\gamma$, were examined. It was also found that the variation of $dC_m'/d\gamma$ with collective blade angle was negligible for the range of collective blade angles examined; hence, a single curve was defined for all of the collective blade angles.

Propeller Blade Stresses

As noted in the foregoing discussion of figures 9 and 10, for a given increment in monocyclic blade angle a greater pitching-moment change can be produced on the rigid configuration than on the flapping configuration. However, the blade stresses produced in the propeller also must be considered in the evaluation because the maximum monocyclic blade angle could be limited by these stresses. To determine the variation of propeller blade stresses with monocyclic blade angle for the two configurations, flapwise bending stresses and trailing-edge in-plane tensile stresses were examined at the blade stations where maximum values for each occurred. These stresses were divided by the appropriate allowable stresses and are presented in figures 15 through 17 as stress ratios. Figures 15 and 16 show that for both the flapping and the rigid configuration the variations of the steady stress ratios with monocyclic blade angle were small, regardless of collective blade angle.

Figures 17(a) and (b) show the oscillatory stress ratios and phase angles in polar form for the flapping and the rigid configuration, respectively. The results presented are for zero free-stream velocity, 12° collective blade angle, and the first two harmonics only. At the other test conditions the variation of the oscillatory stress ratios with monocyclic blade angle remained essentially the same with only the magnitude of the minimum stress ratio varying slightly (less than 0.1). For this reason the oscillatory stress ratios obtained at the other test conditions are not presented. It was also found that the major variations in the stresses for the two configurations occurred in the first two harmonics; hence, only these are presented.

It is apparent from figure 17 that the oscillating stress ratio variations with monocyclic blade angle are different for the two configurations. For the rigid configuration the once-per-revolution oscillatory flapwise bending stress was about 4 to 5 times more sensitive to changes in monocyclic blade angle than for the flapping configuration. The twice-per-revolution oscillatory trailing-edge or chordwise bending stress of the flapping configuration was about 3 to 4 times more sensitive to changes in monocyclic blade angle than the rigid configuration.

QUALITATIVE REMARKS

The rates of oscillatory stress rise with monocyclic blade angle, indicated by the results, suggest that these stresses could be the limiting factor on the amount of control or trim that could be realized. Indeed, if this propeller, in either its rigid or flapping configuration, was used on the VZ-2 airplane for which it was designed, its trim and control capabilities would be less than that of the aft pitch fan which was installed on the airplane. Since the control capabilities of this fan in hover (ref. 2) have been shown to be nearly 30 percent deficient (see ref. 3), it is obvious that the monocyclic control would be unsatisfactory for this application. It should be noted, however, that a stronger propeller of either configuration could be constructed to withstand the applied loads. For example, propeller number 1 of reference 1 (a rigid propeller) could

be scaled to the size of the test propeller. The yawing moment generated by this propeller in pitch attitude (ref. 1), which is analogous to monocyclic variation of the blade angle, was as much as 8,000 ft/lb without exceeding the allowable blade stress. To provide sufficient pitching-moment control for the VZ-2 airplane, about 2,000 ft/lb of moment would be required. This would be equivalent to about 7° of monocyclic blade angle variation for the scaled down rigid propeller being considered. A considerable increase in propeller weight would result, however, and must be considered in this approach.

In summary, the test results indicate that, generally, the rigid propeller configuration would be more effective than the flapping configuration as a means of longitudinal trim and control. The stresses produced by the monocyclic blade angle variation must be considered in the design of the propeller, and the merit of this method of generating control moments in comparison with other means must be based upon the peculiarities of the individual installation.

Ames Research Center
National Aeronautics and Space Administration
Moffett Field, Calif., Feb. 21, 1963

REFERENCES

1. Yaggy, Paul F., and Rogallo, Vernon L.: A Wind-Tunnel Investigation of Three Propellers Through an Angle-of-Attack Range From 0° to 85°. NASA TN D-318, 1960.

2. Pegg, Robert J.: Summary of Flight-Test Results of the VZ-2 Tilt-Wing Aircraft. NASA TN D-989, 1962.

3. Reeder, John P.: Handling Qualities Experience With Several VTOL Research Aircraft. NASA TN D-735, 1961.

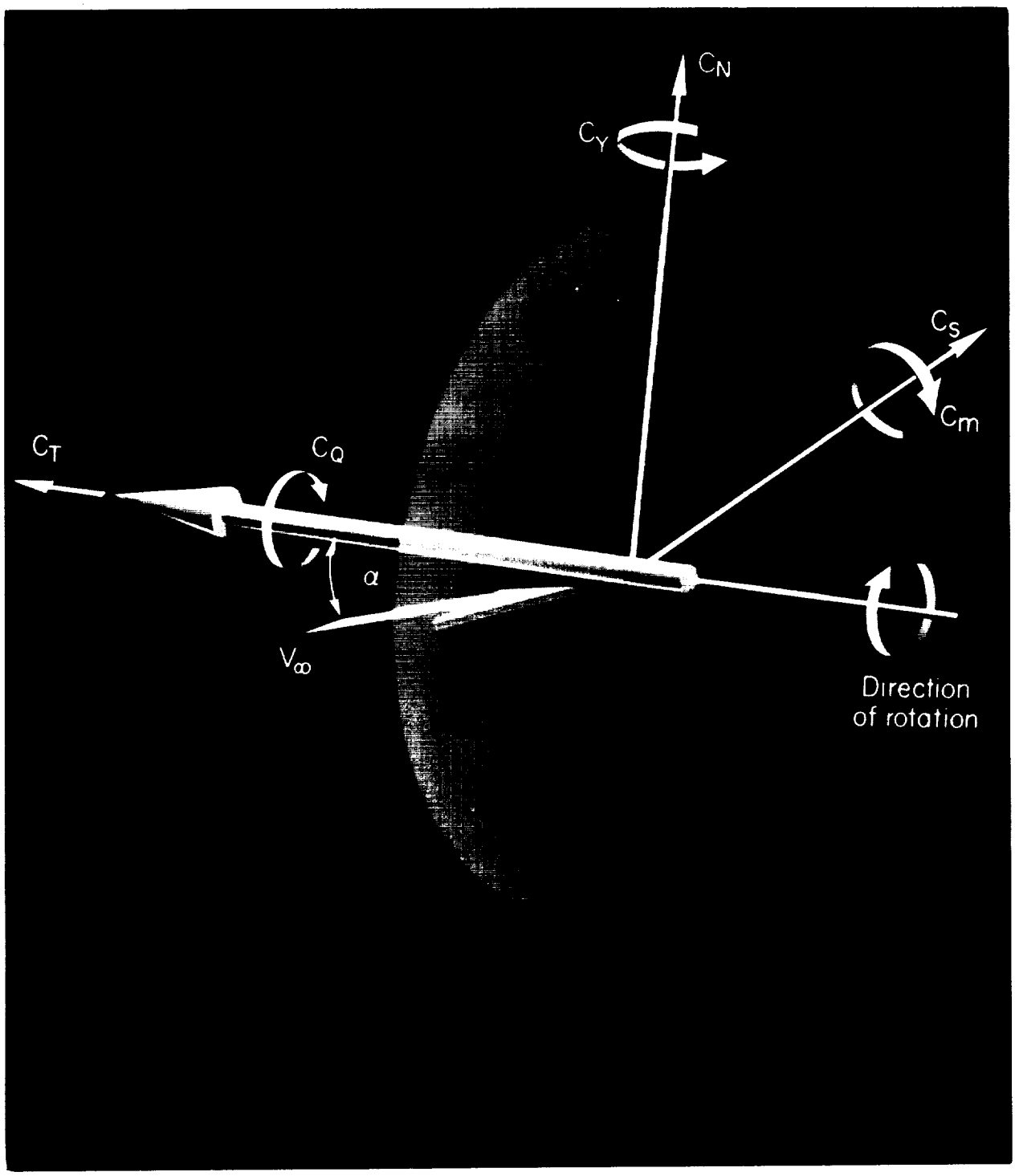

A-28486

Figure 1.- Positive directions of propeller forces and moments.

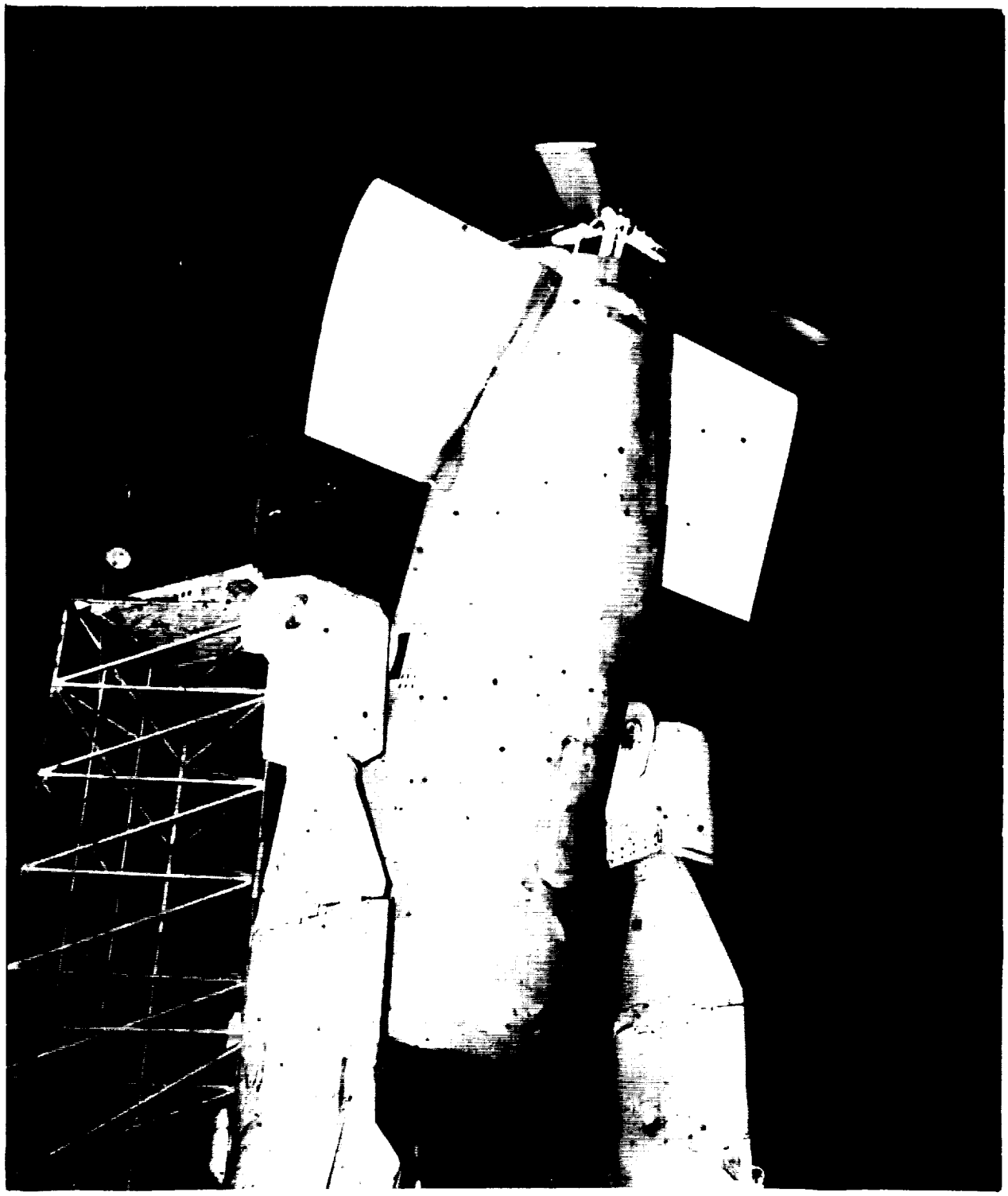

A-26029

Figure 2.- Propeller and test stand with wing installed in the Ames 40- by 80-Foot Wind Tunnel.

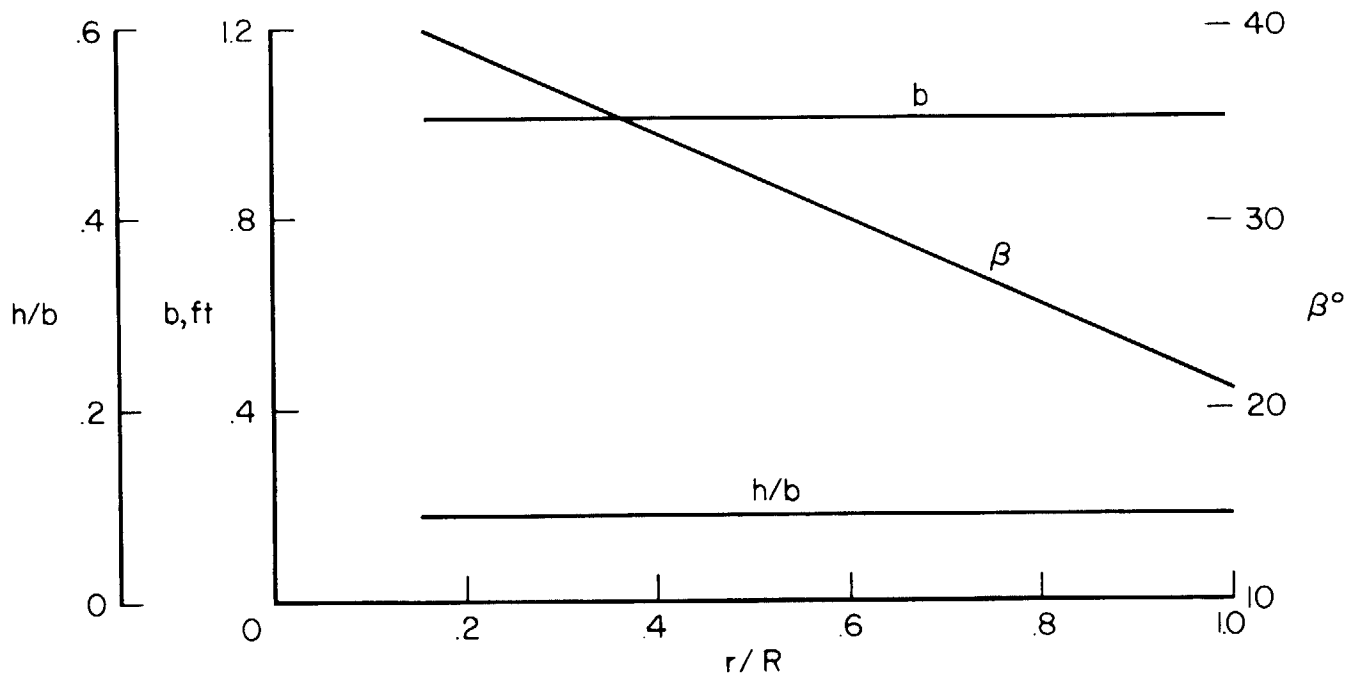

Figure 3.- Propeller blade plan-form characteristics.

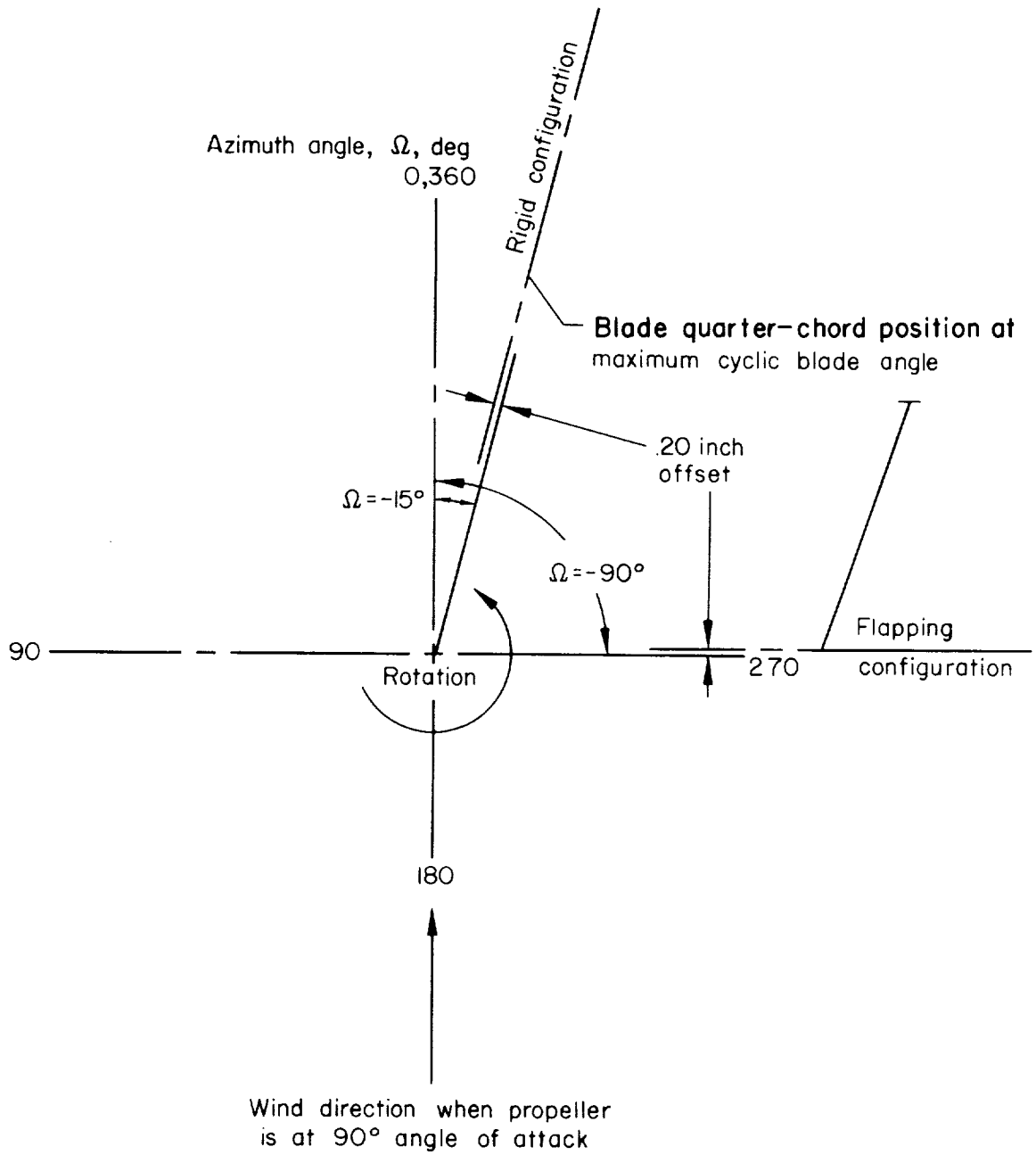

Figure 4.- Plan view showing azimuth angle at which the maximum monocyclic blade angle occurs for the two configurations.

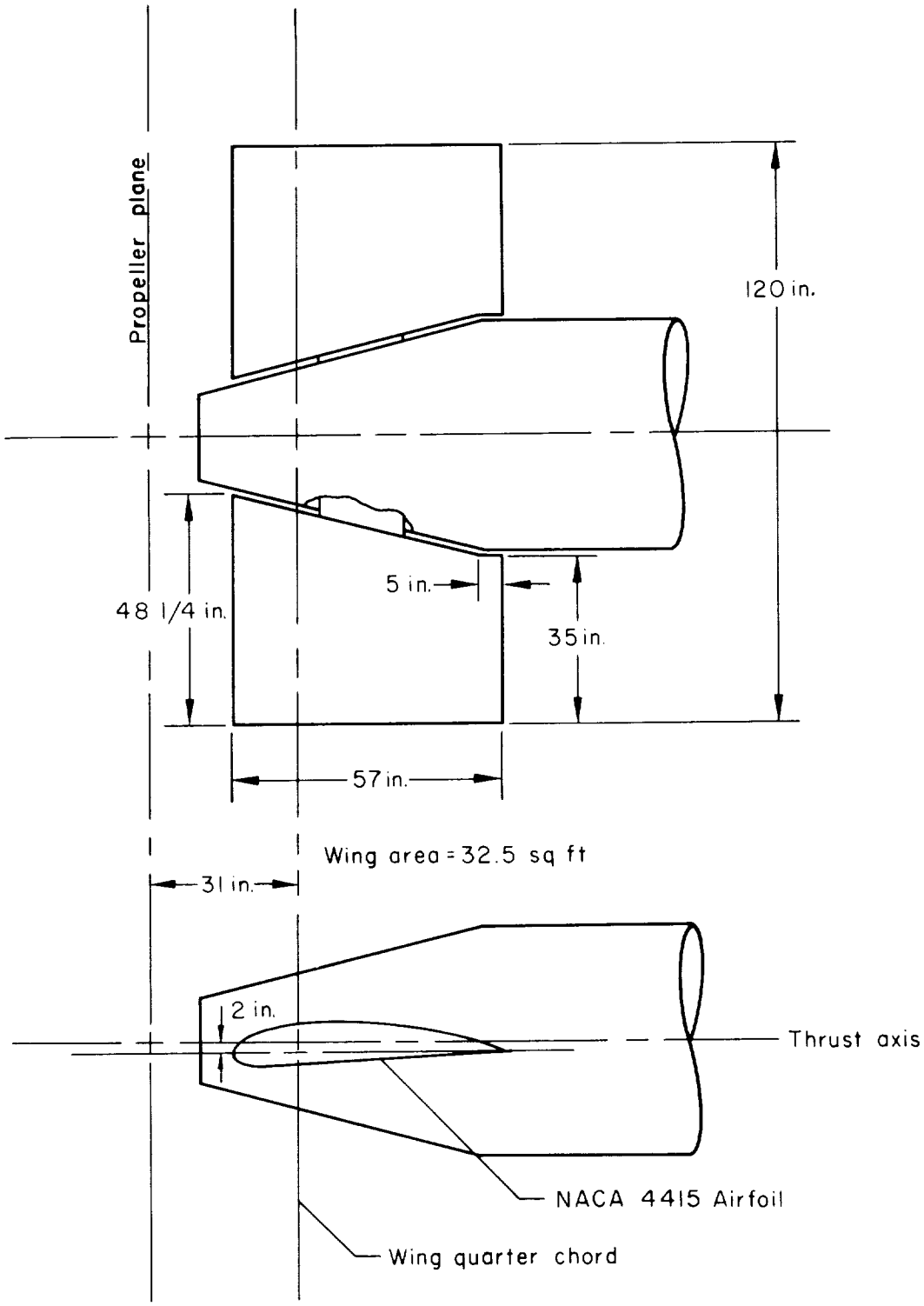

Figure 5.- Details of the wing dimensions and mounting position.

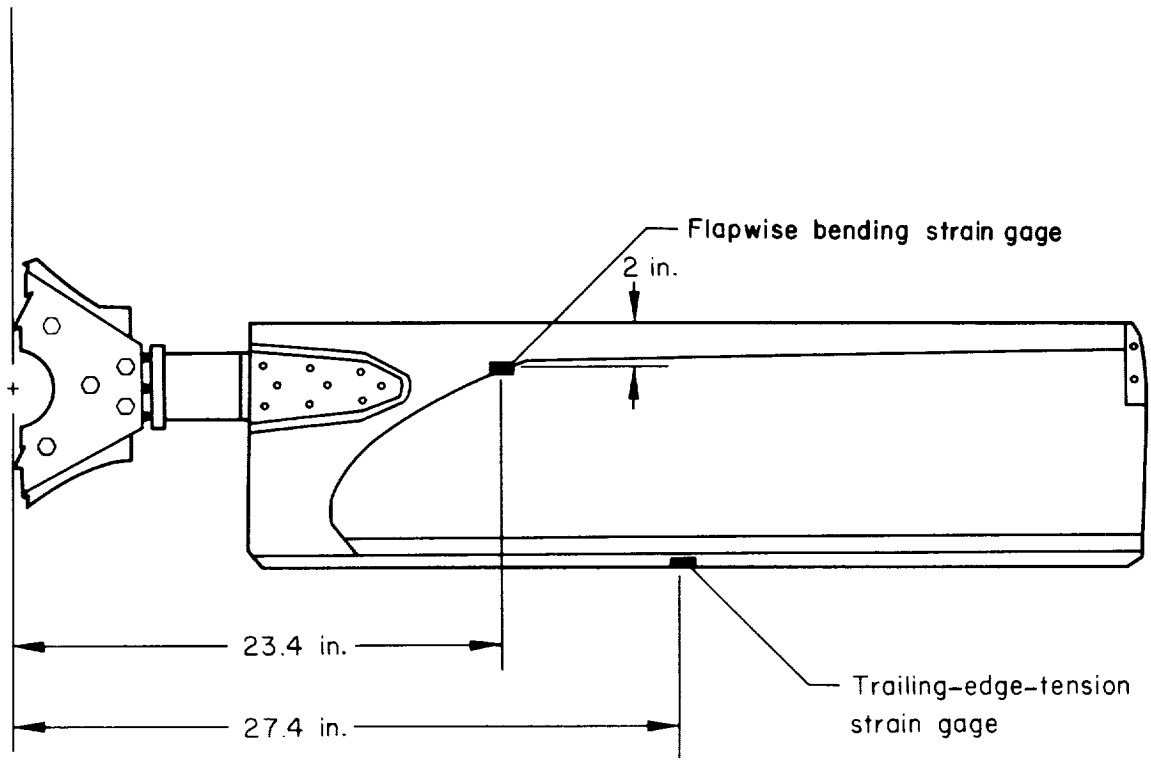

Figure 6.- Position of blade strain gages.

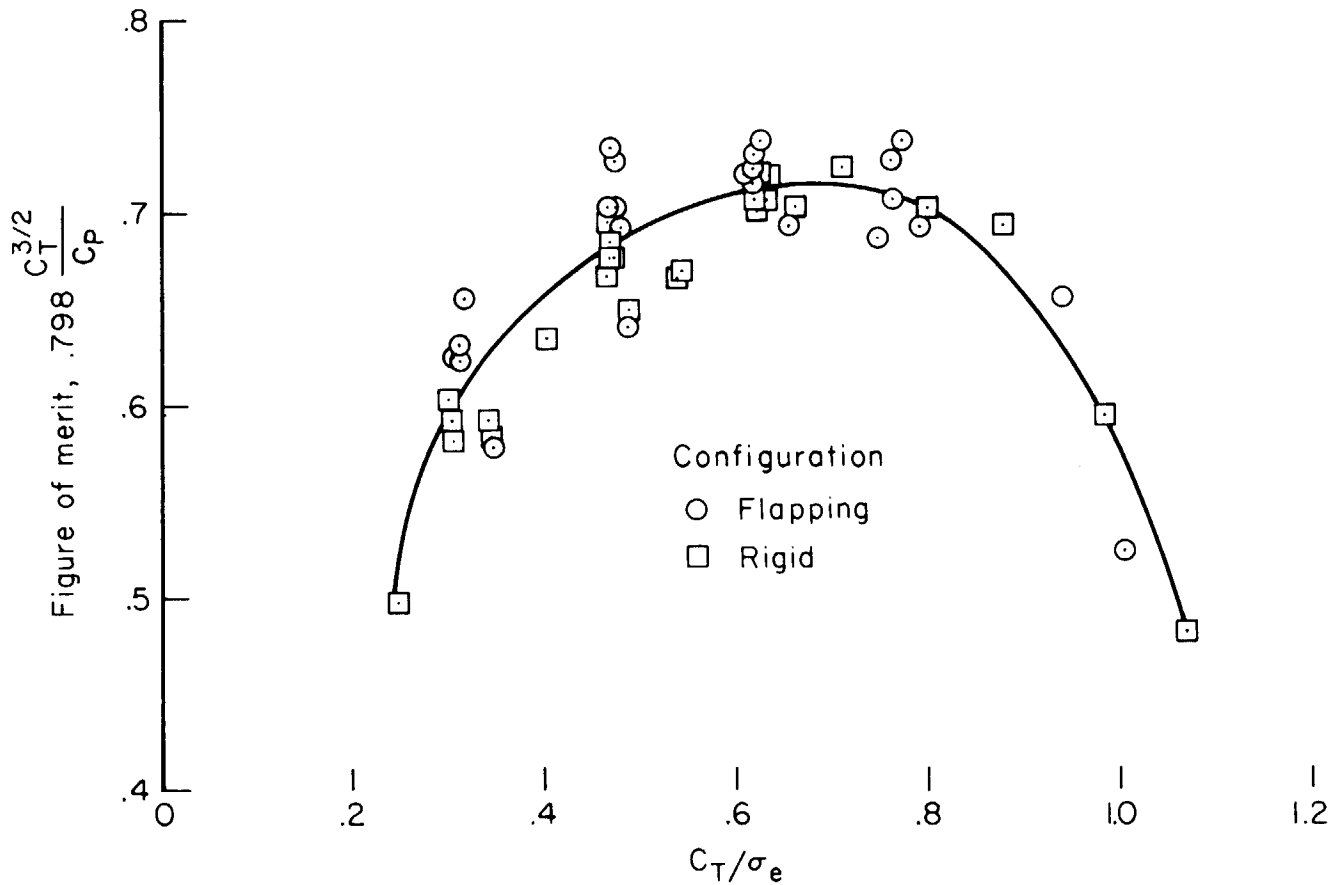

Figure 7.- Figure of merit as a function of weighted thrust coefficient for the two configurations; $V_\infty = 0$.

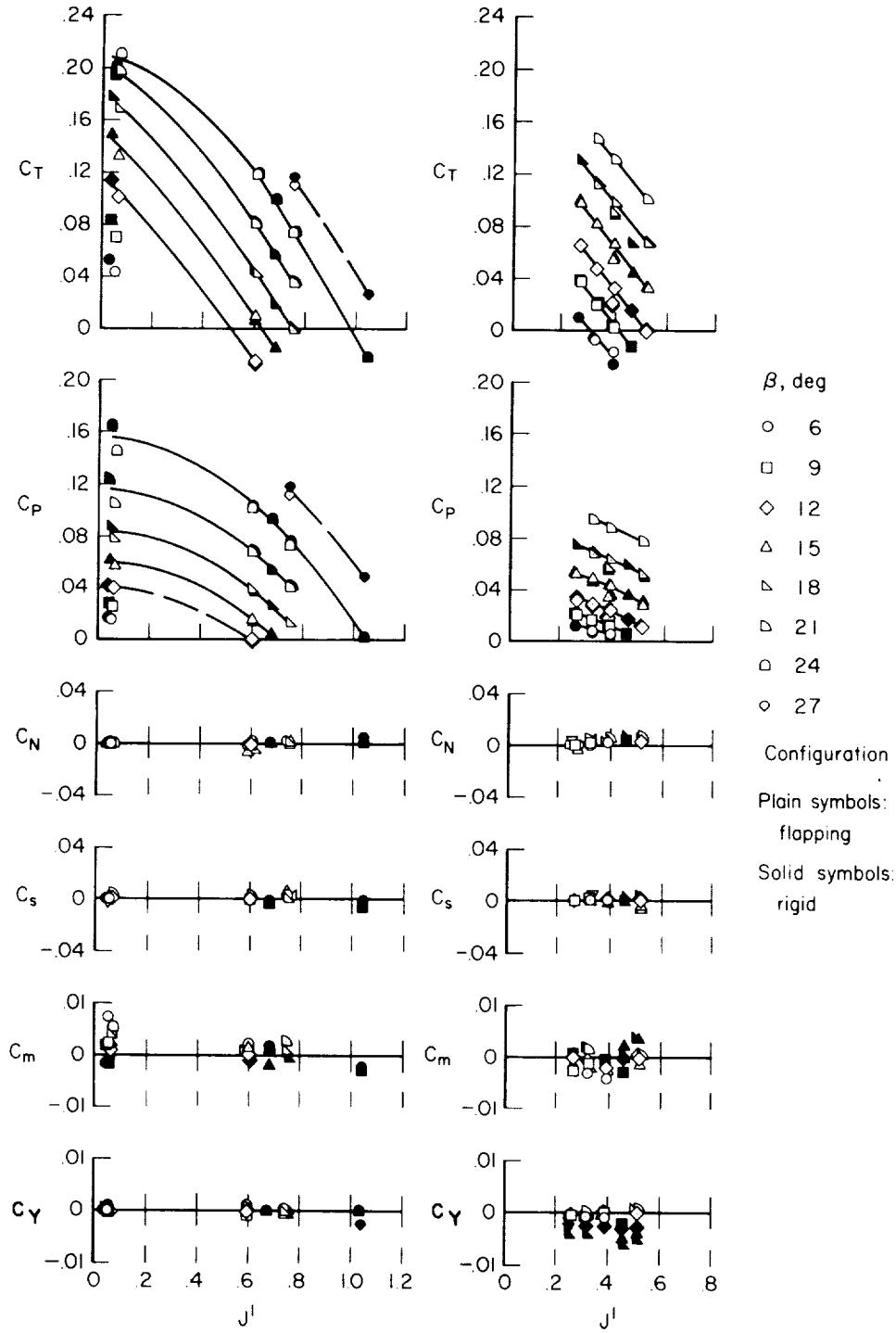

(a) $\alpha = 0^{\circ}$ (b) $\alpha = 30^{\circ}$

Figure 8.- Aerodynamic characteristics of the two configurations at four angles of attack; n = 23.5 rps.

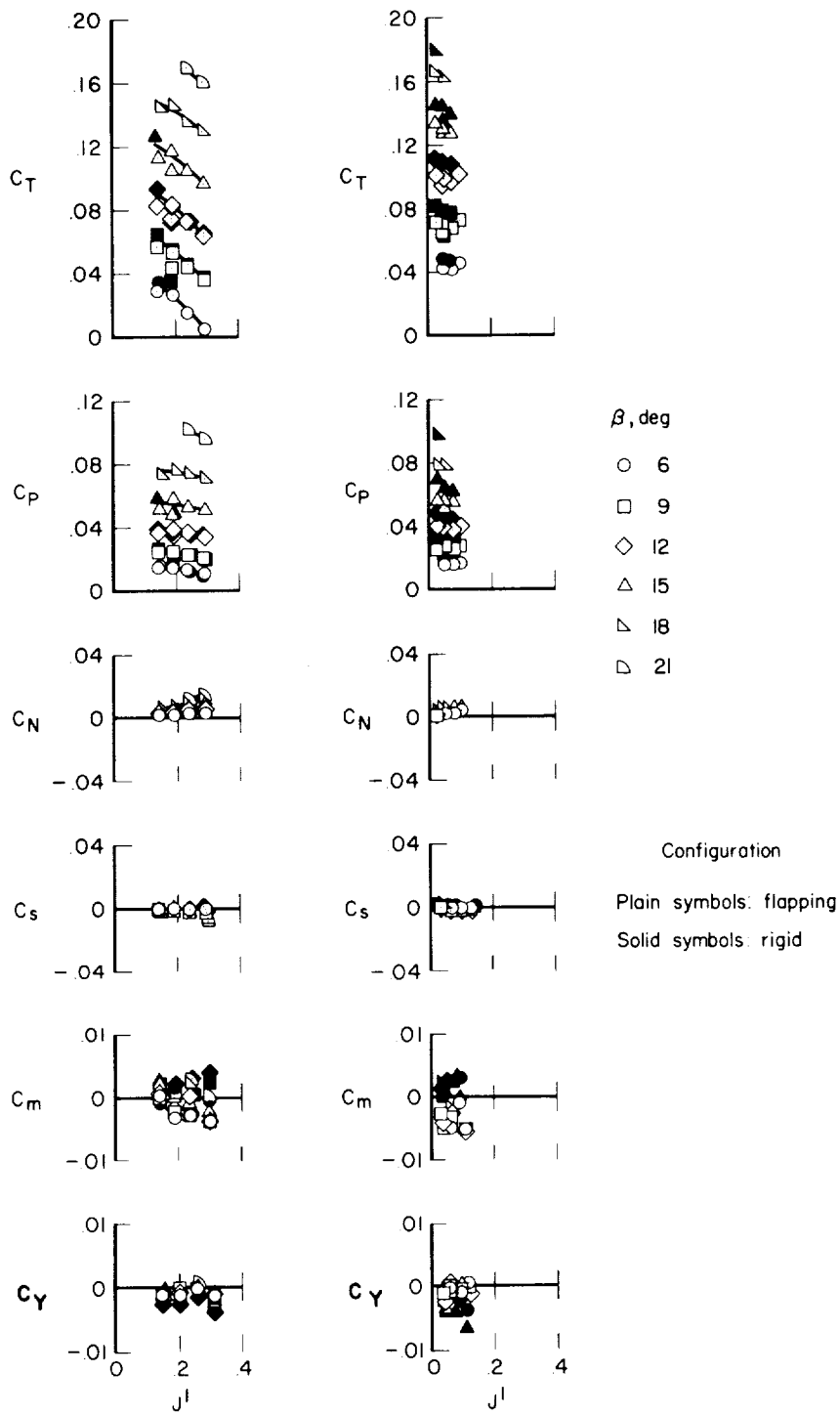

(c) a = 50° (d) α = 70°

Figure 8.- Concluded.

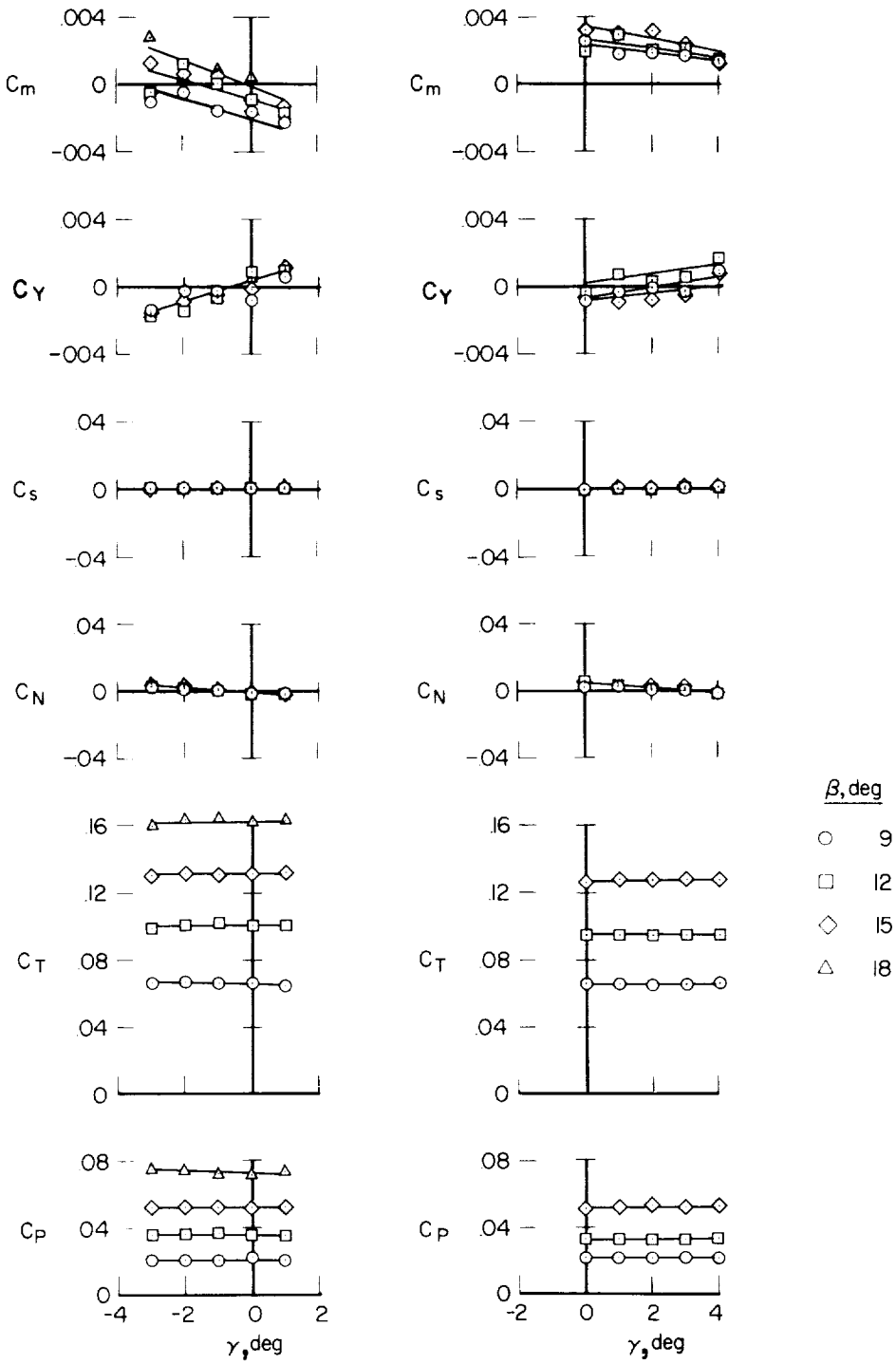

(a) V_∞ = 0 knots; α = 85° (b) V_∞ = 20 knots; α = 70°

Figure 9.- The effects of monocyclic blade angle variation on the aerodynamic characteristics of the flapping configuration for four combinations of angle of attack and free-stream velocity.

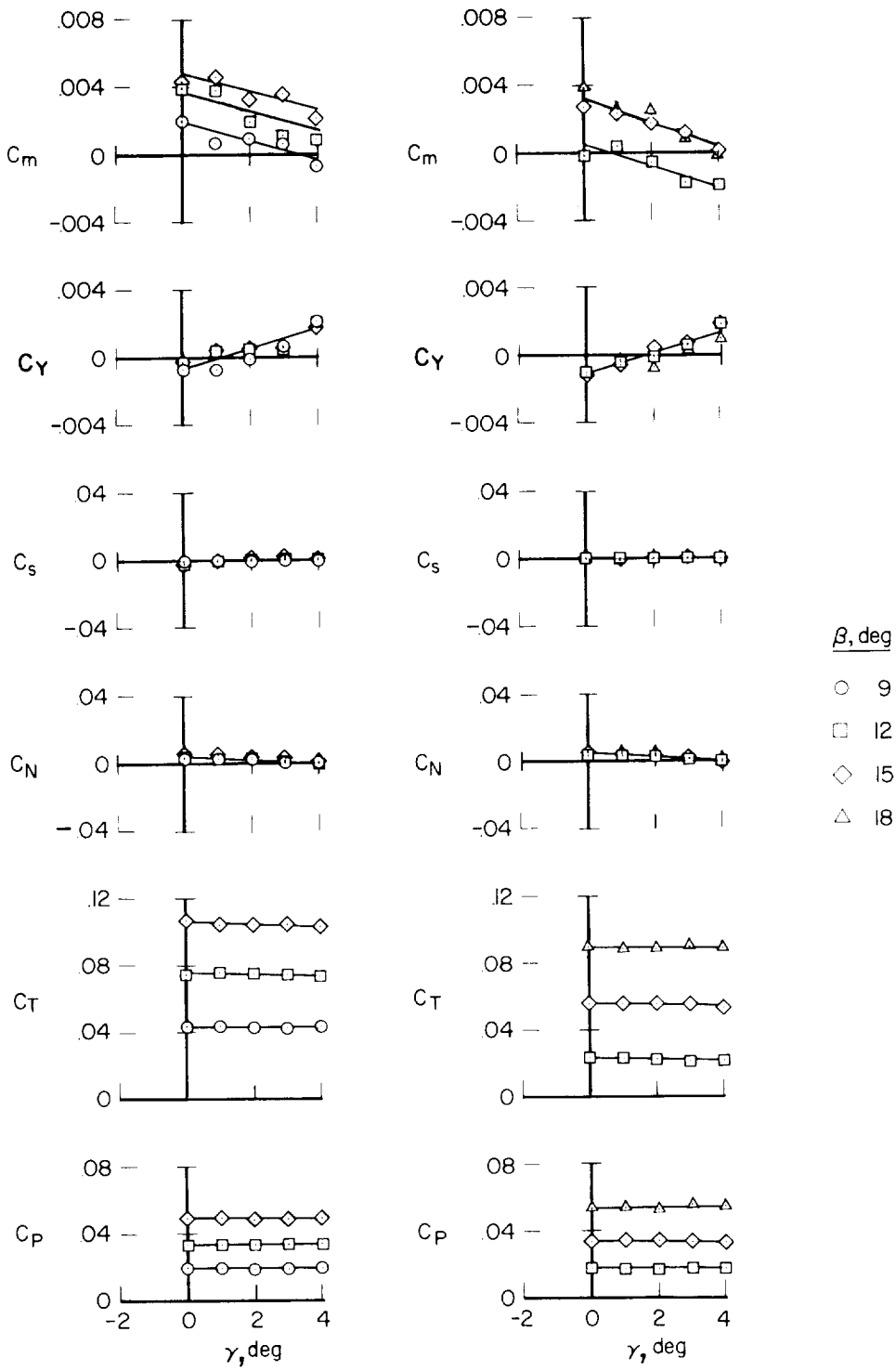

(c) V_∞ = 40 knots; α = 50° (d) V_∞ = 60 knots; α = 30°

Figure 9.- Concluded.

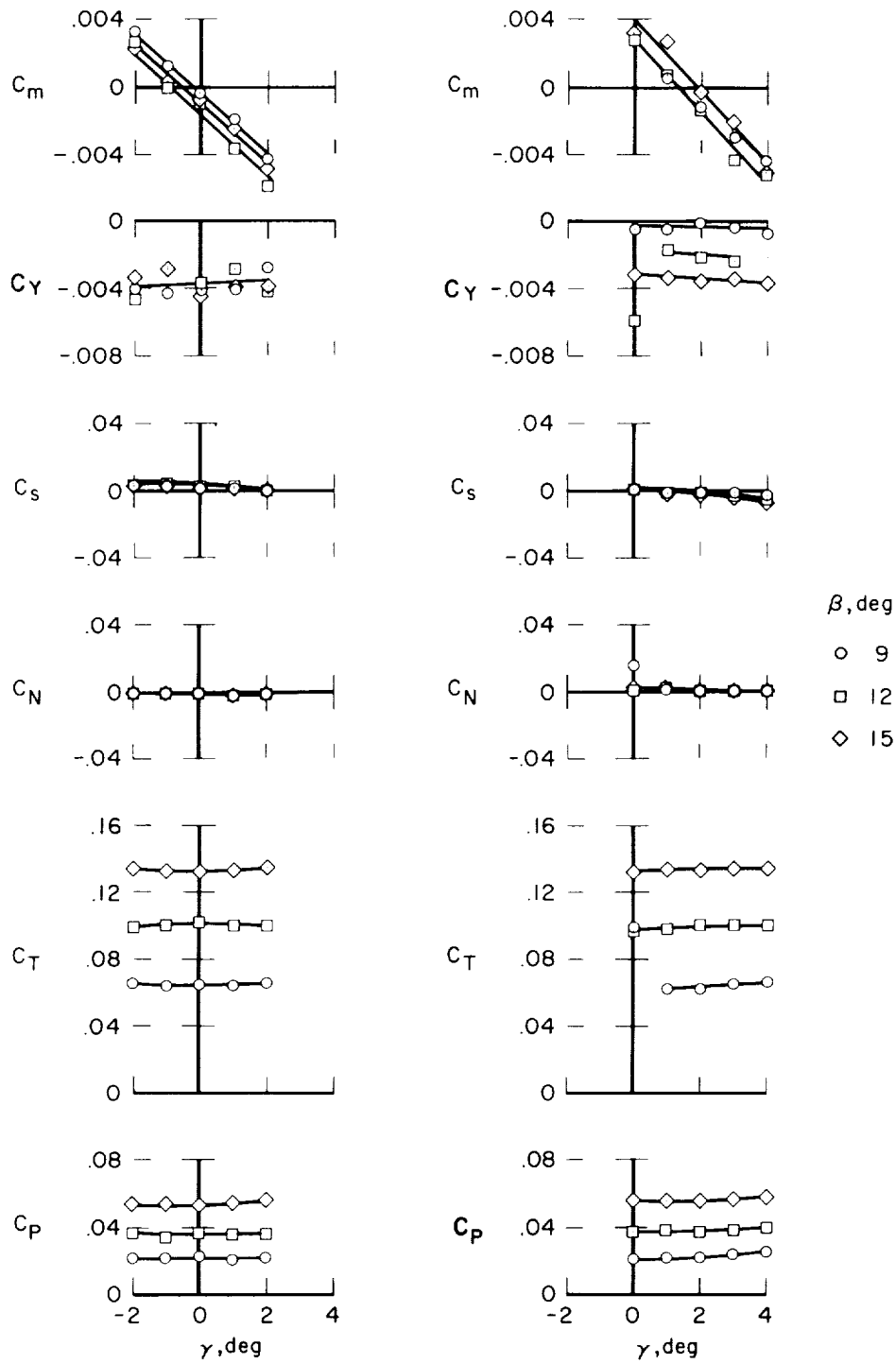

(a) V_∞ = 0 knots; α = 85° (b) V_∞ = 20 knots; α = 70°

Figure 10.- The effect of monocyclic blade angle variation on the aerodynamic characteristics of the rigid configuration for four combinations of angle of attack and free-stream velocity.

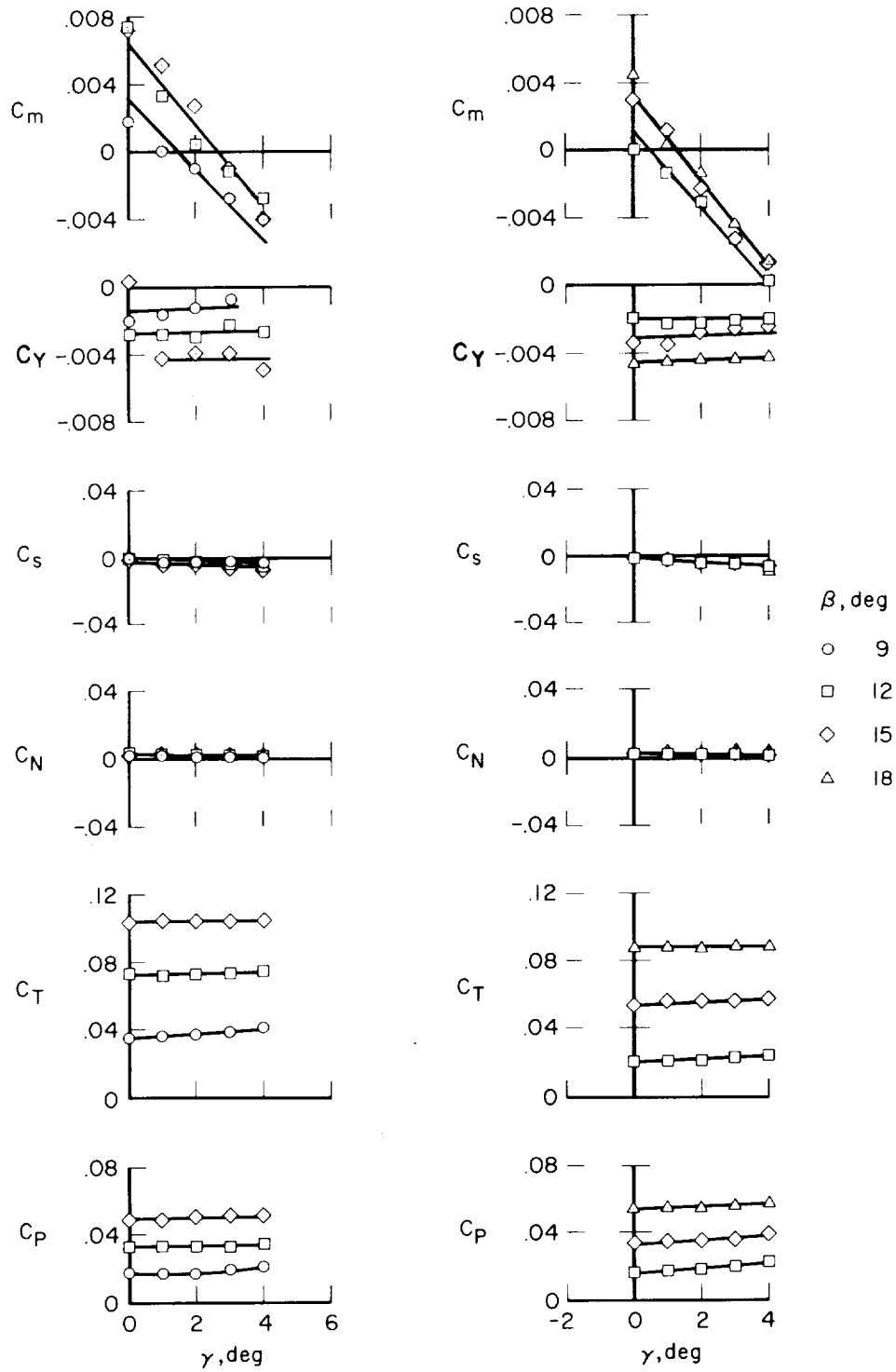

(c) V_∞ = 40 knots; α = 50° (d) V_∞ = 60 knots; α = 30°

Figure 10.- Concluded.

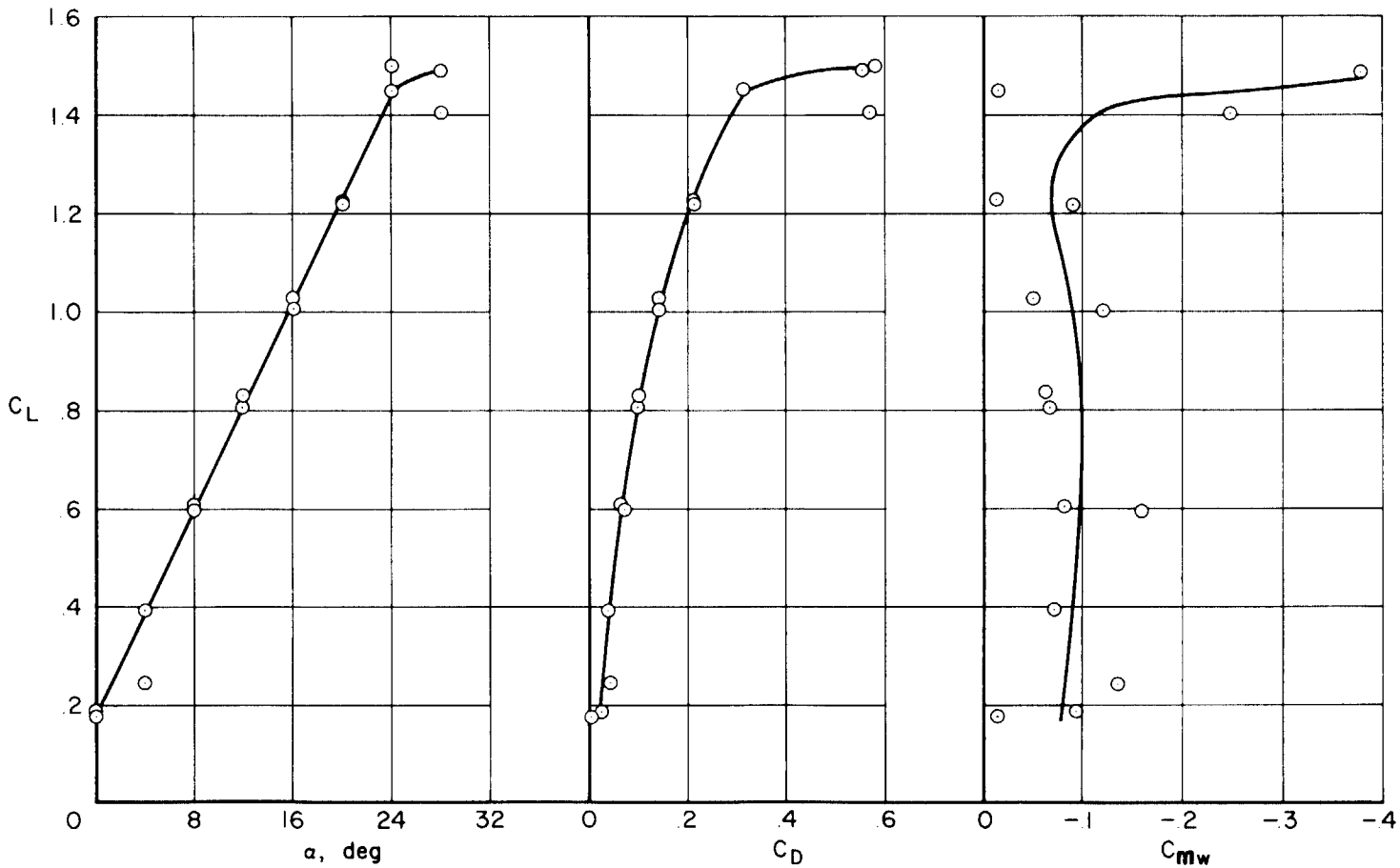

Figure 11.- Aerodynamic characteristics of wing alone.

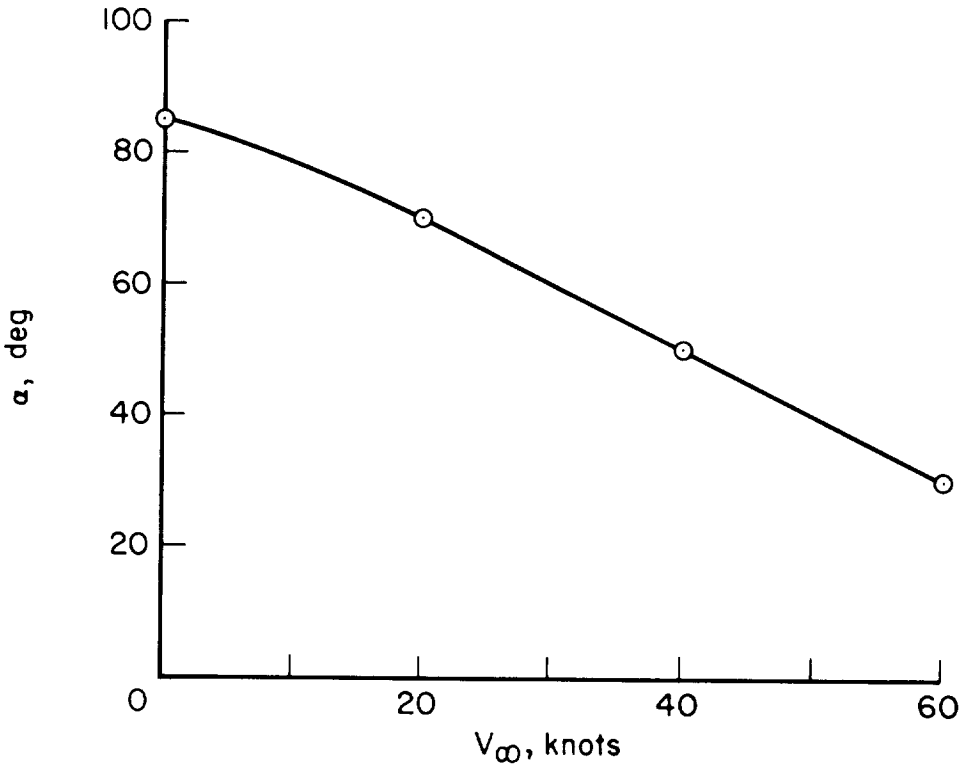

(a) Angle of attack at which $dC_m/d\gamma$ examined.

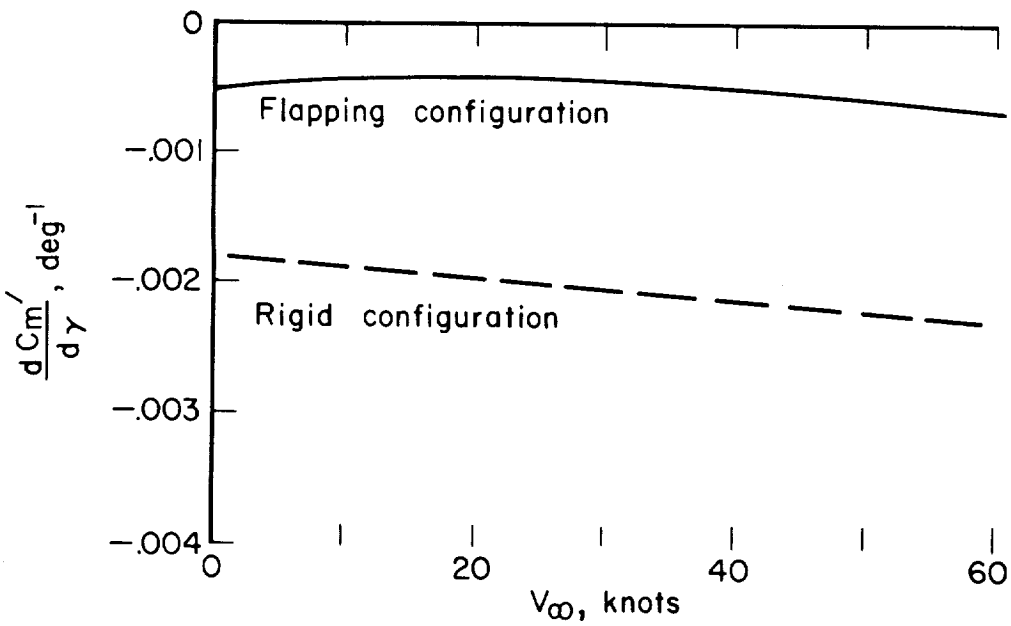

(b) Center of gravity located at the propeller hub; wing off.

Figure 12.- Examination of $dC_m'/d\gamma$ with the wing on and off for two center-of-gravity locations and for both propeller configurations.

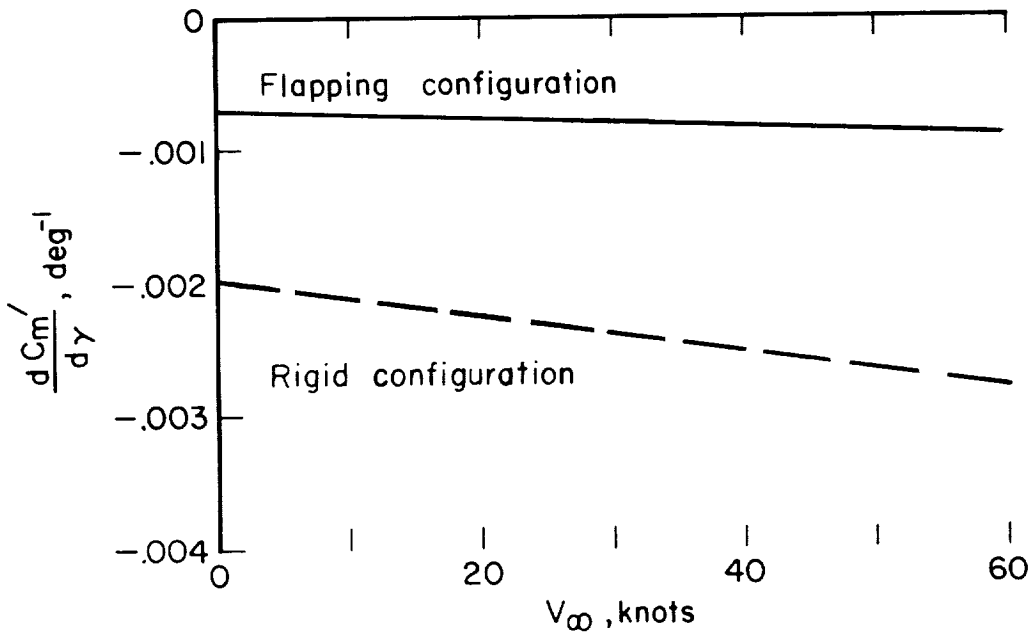

(c) Center of gravity located at the wing quarter chord; wing off.

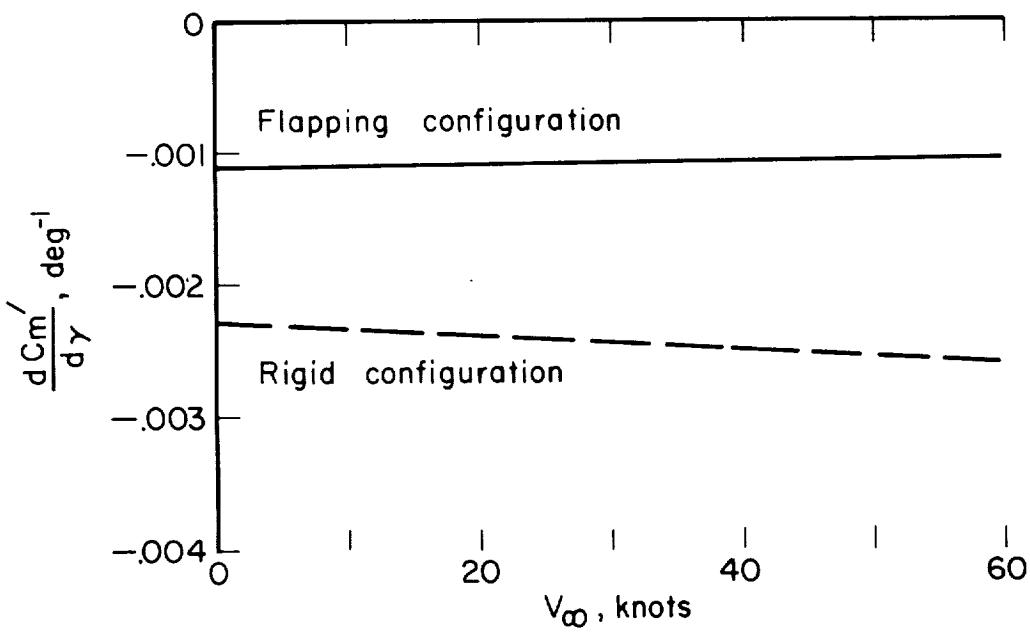

(d) Center of gravity located at the wing quarter chord; wing on.

Figure 12.- Concluded.

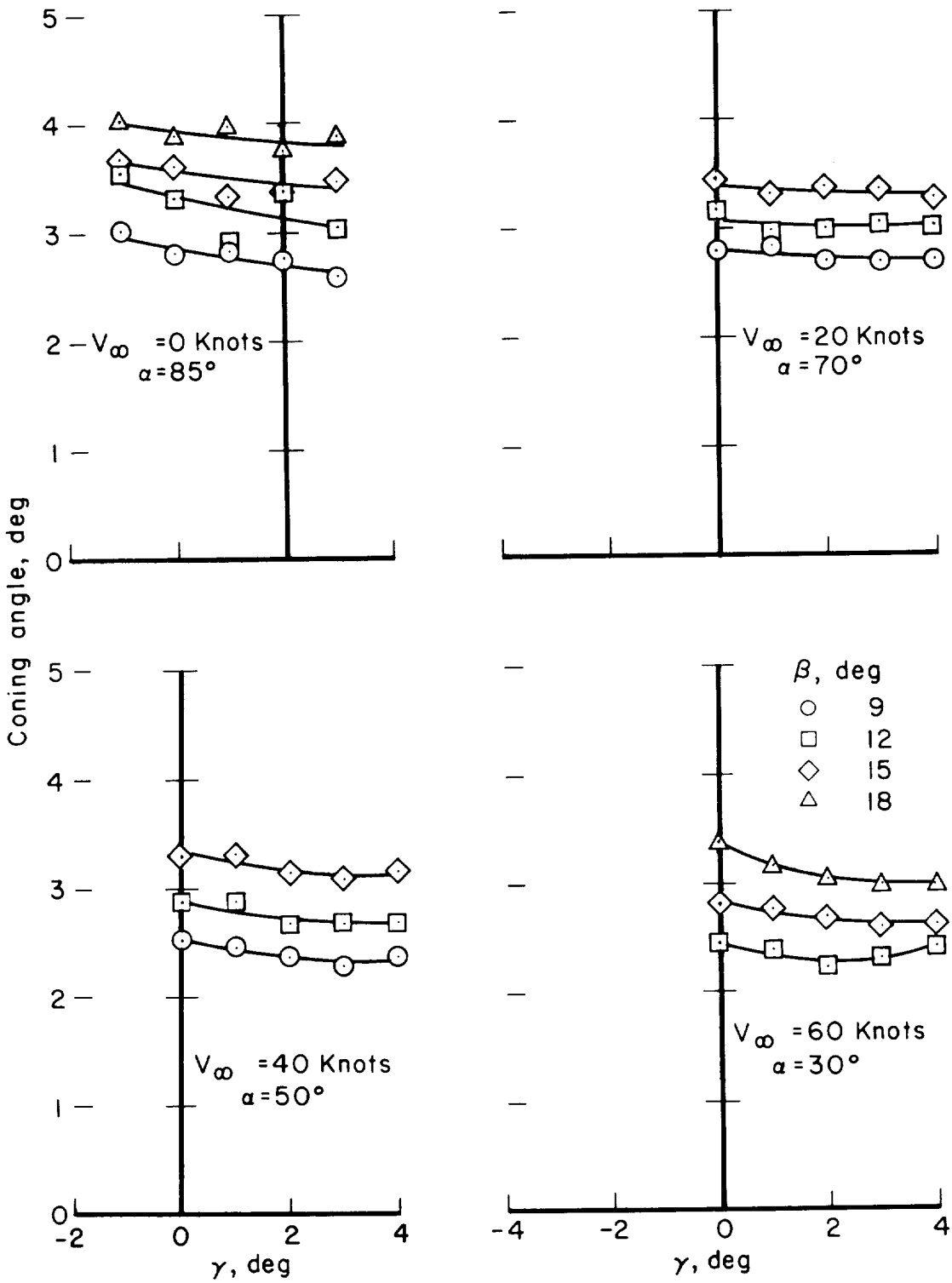

Figure 13.- Effect of monocyclic blade angle variation on the coning angle measured with respect to the plane of rotation; positive upstream.

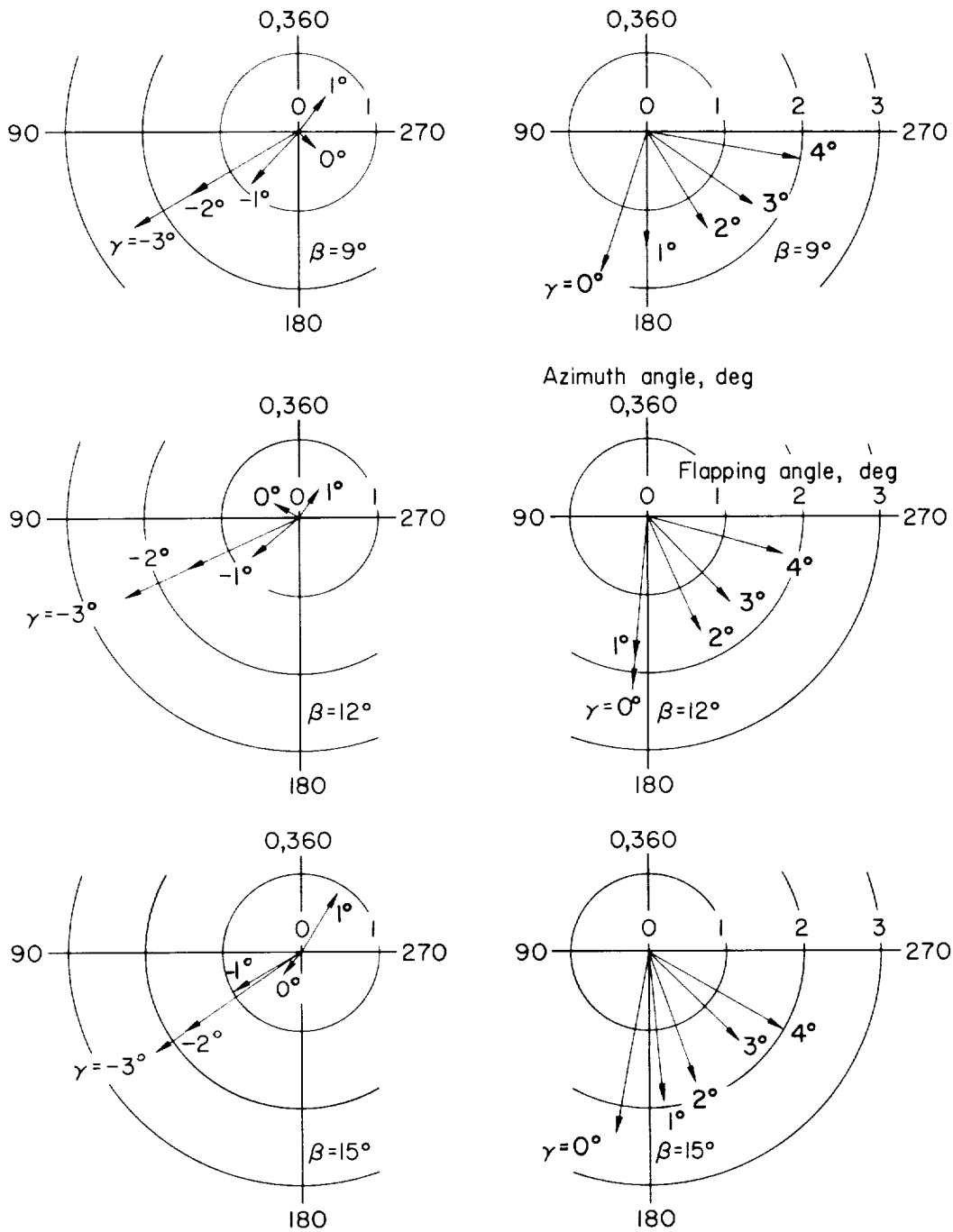

(a) V_∞ = 0 knots; α = 85° (b) V_∞ = 20 knots; α = 70°

Figure 14.- Effect of monocyclic blade angle variation on the flapping angle measured with respect to the coning angle; positive upstream.

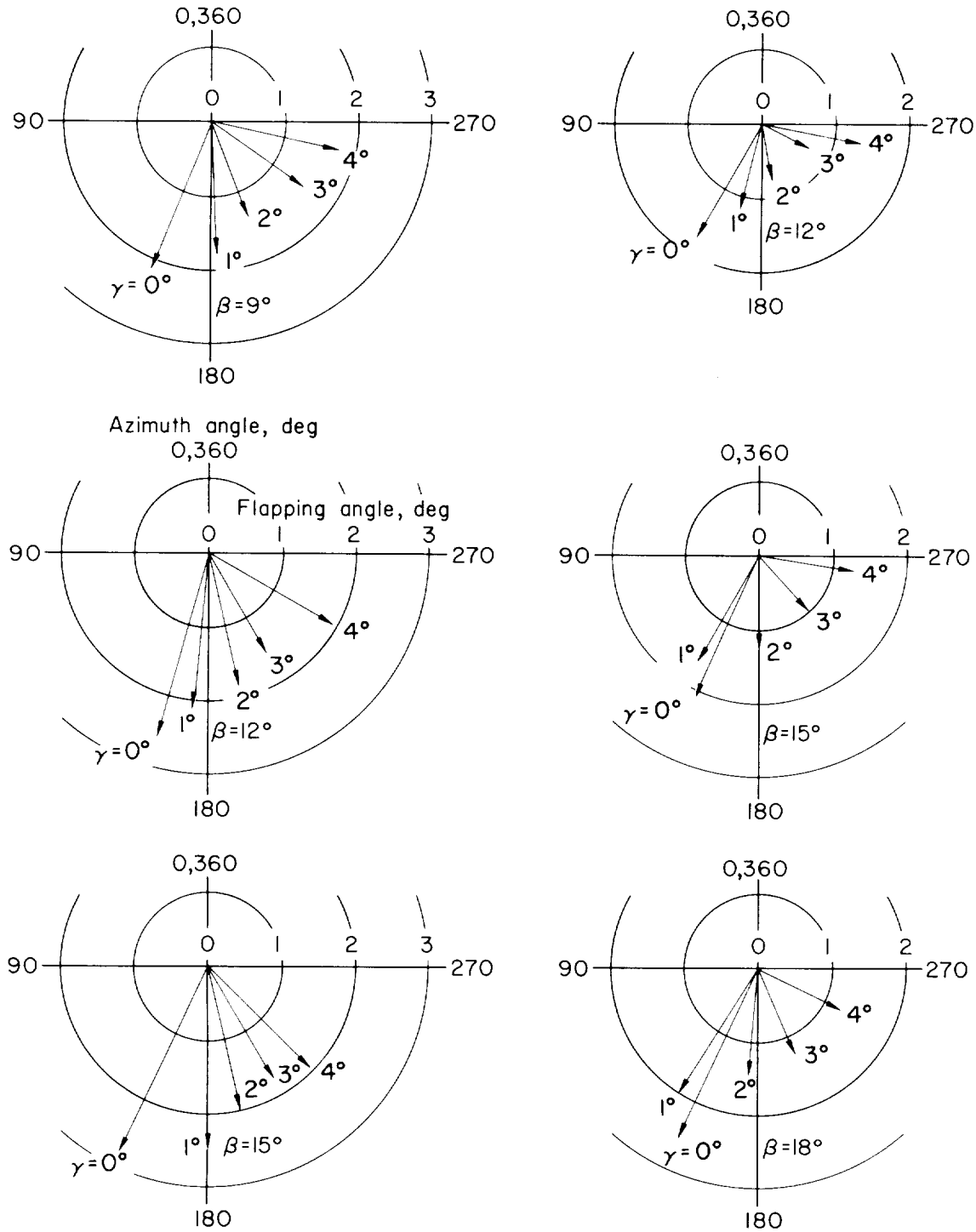

(c) V_∞ = 40 knots; α = 50°

(d) V_∞ = 60 knots, α = 30°

Figure 14.- Concluded.

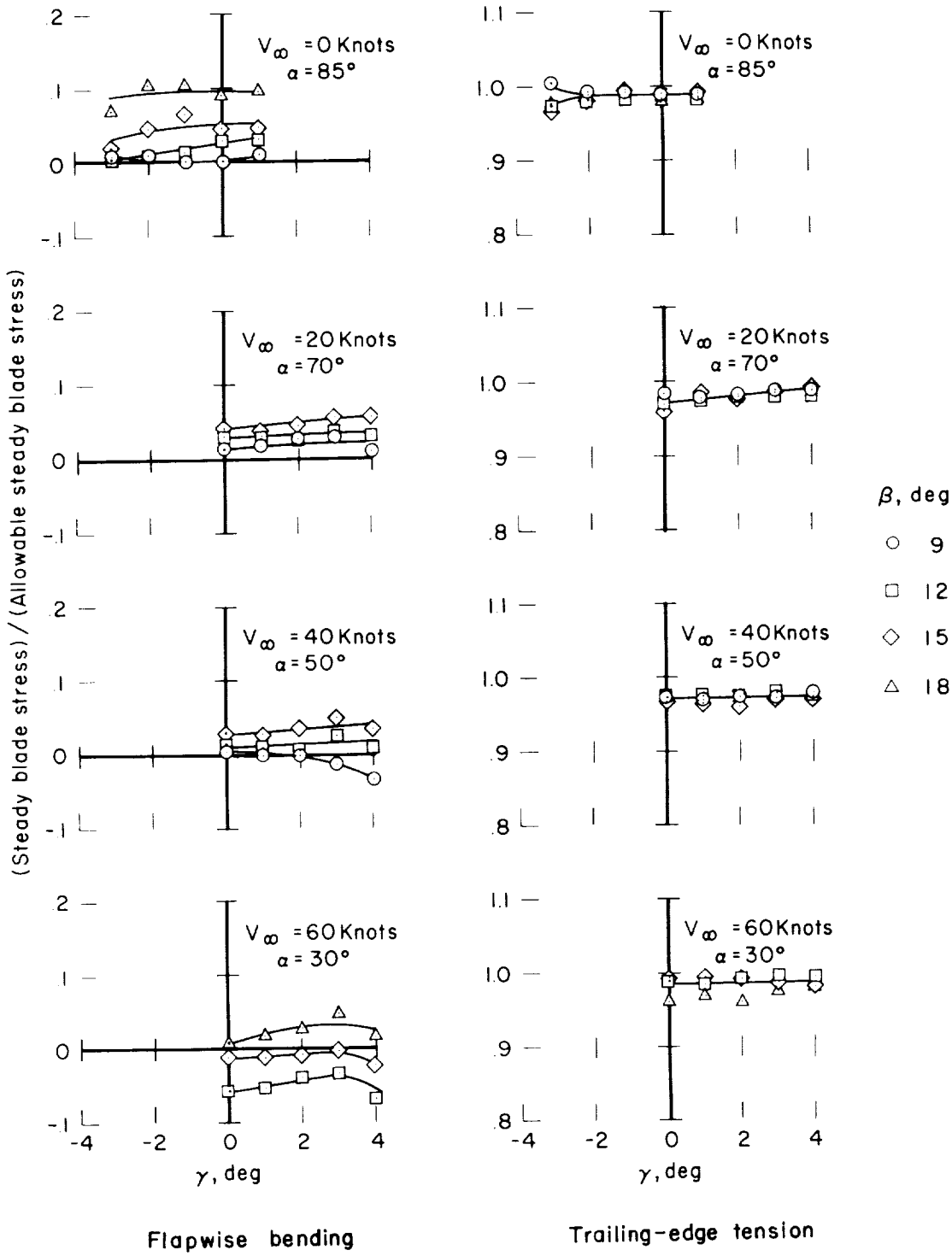

Figure 15.- Effect of monocyclic blade angle variation on the steady blade stress ratios for the flapping configuration; positive stress ratio if blade is bending forward.

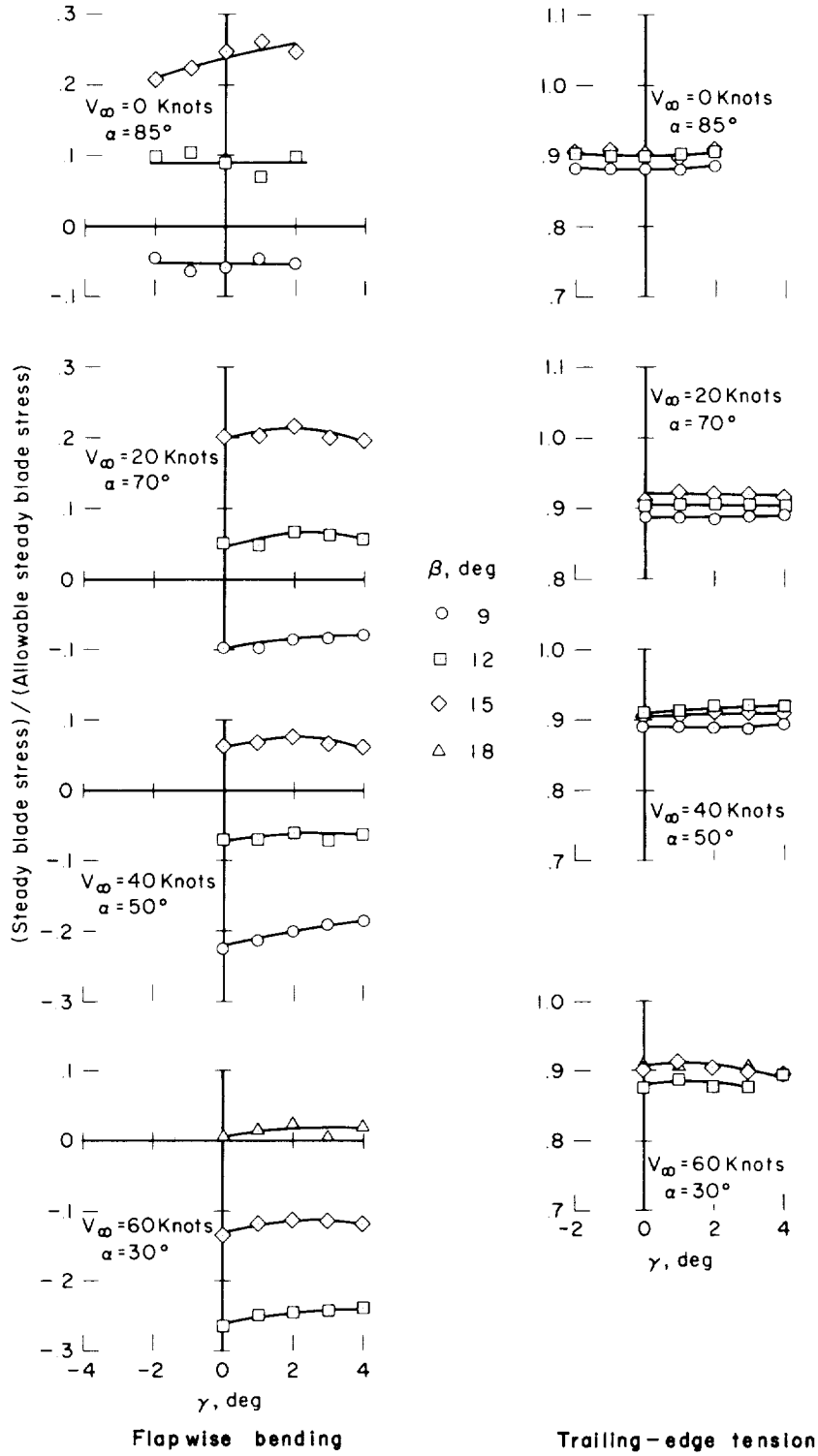

Figure 16.- Effect of monocyclic blade angle variation on the steady blade stress ratios for the rigid configuration; positive stress ratio if blade is bending forward.

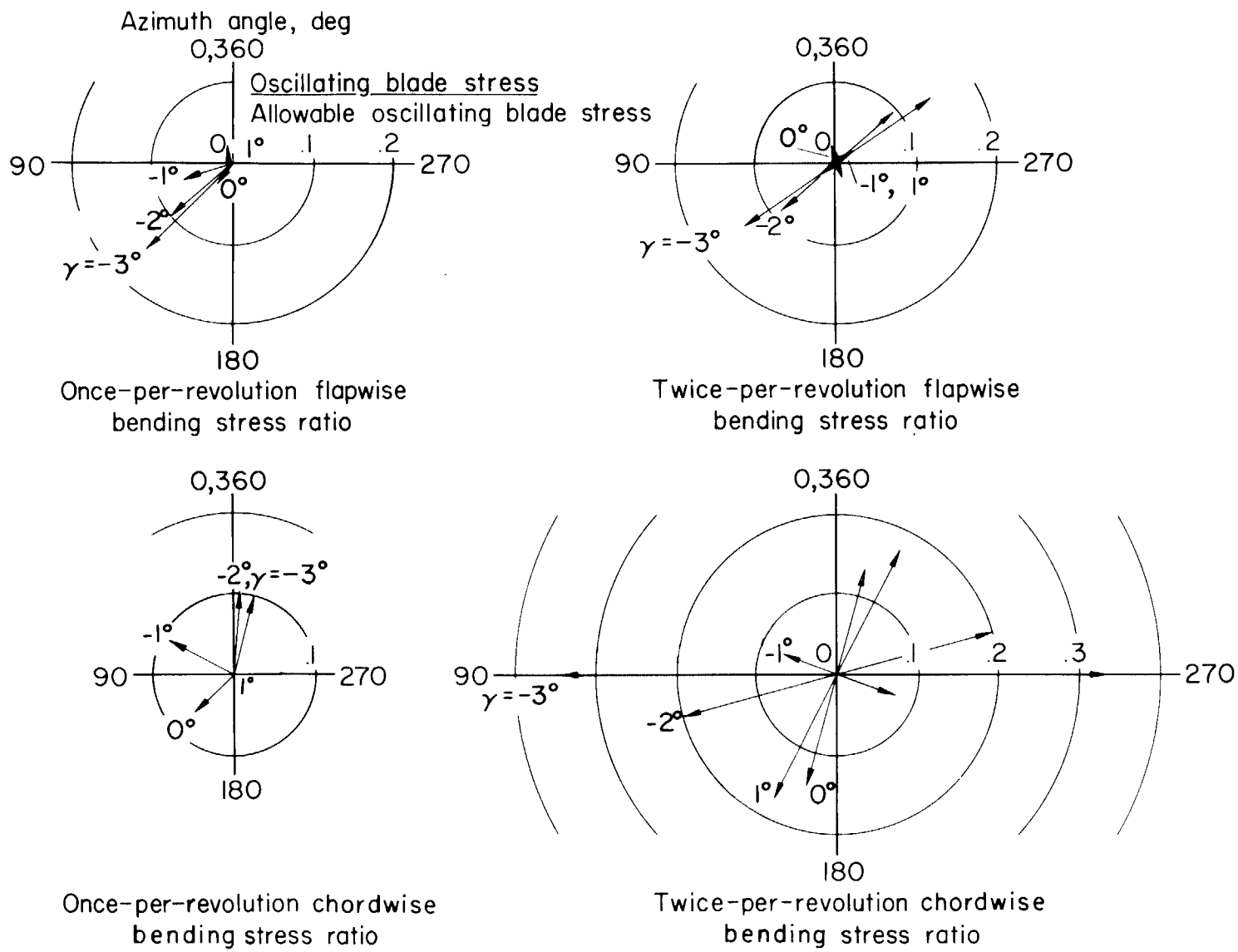

(a) Flapping configuration.

Figure 17.- Effect of monocyclic blade angle variation on the oscillating blade stress ratios for the first two harmonics at $V_\infty = 0$ knots and $\beta = 12^\circ$.

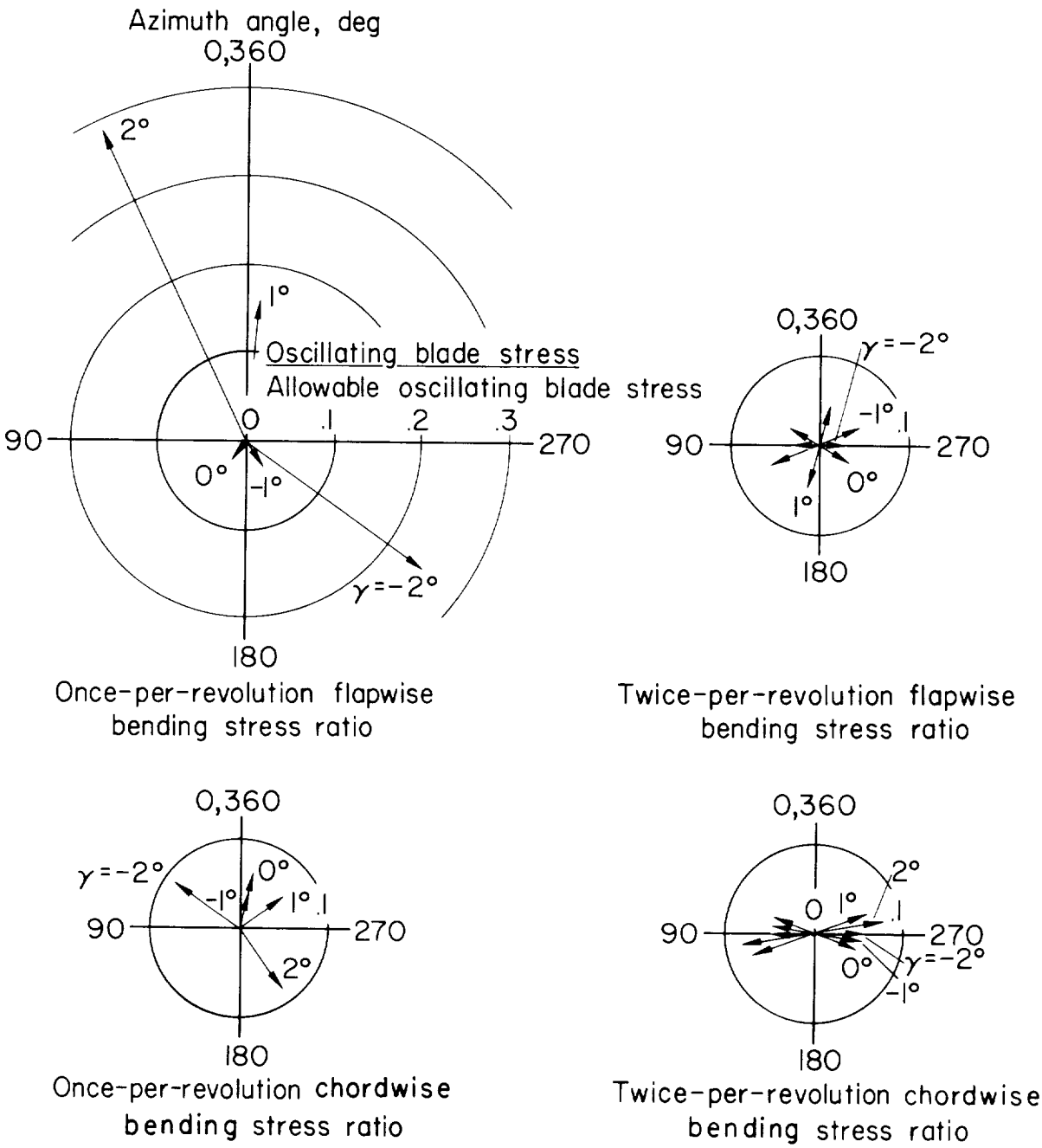

(b) Rigid configuration.

Figure 17.- Concluded.